



HAL
open science

Intensification potential of hollow fiber membrane contactors for CO₂ chemical absorption and stripping using monoethanolamine solutions

David Albarracin Zaidiza, Bouchra Belaisaoui, Sabine Rode, Eric Favre

► **To cite this version:**

David Albarracin Zaidiza, Bouchra Belaisaoui, Sabine Rode, Eric Favre. Intensification potential of hollow fiber membrane contactors for CO₂ chemical absorption and stripping using monoethanolamine solutions. Separation and Purification Technology, 2017, 188, pp.38-51. 10.1016/j.seppur.2017.06.074 . hal-02943291

HAL Id: hal-02943291

<https://hal.science/hal-02943291>

Submitted on 28 Apr 2024

HAL is a multi-disciplinary open access archive for the deposit and dissemination of scientific research documents, whether they are published or not. The documents may come from teaching and research institutions in France or abroad, or from public or private research centers.

L'archive ouverte pluridisciplinaire **HAL**, est destinée au dépôt et à la diffusion de documents scientifiques de niveau recherche, publiés ou non, émanant des établissements d'enseignement et de recherche français ou étrangers, des laboratoires publics ou privés.

Intensification Potential of Hollow fiber Membrane Contactors for CO₂ Chemical Absorption and Stripping using Monoethanolamine solutions

David Albarracin Zaidiza, Bouchra Belaissaoui*, Sabine Rode, Eric Favre

Laboratoire reaction et Génie des procédés (LRGP) (UMR 7274), université de Lorraine, ENSIC, 1, rue Grandville – BP 20451, 54001 Nancy Cedex, France

Manuscript to be submitted to *Separation & Purification Technology*

Jun 2017

*Corresponding author: Tel: +33 372 74 37 98; fax : +33 383 32 29 75
E-mail address: Bouchra.Belaissaoui@univ-lorraine.fr (B.Belaissaoui)

Abstract

In this work, the intensification potential of Hollow fiber membrane contactors (HFMC) for CO₂ capture by chemical absorption using amine solution have been evaluated by simulation, for both absorption and desorption steps. The simulations have been achieved considering typical industrial relevant conditions for post-combustion capture, based on CASTOR campaign at the Esbjerg pilot plant using packed column, operating at its energetic optimum. Rigorous adiabatic 1D simulations are achieved and revealed important temperature variation as well as significant water transmembrane fluxes in both absorber and desorber. Compared to packed column, a contactor volume reduction (i.e. intensification factor) of about 4 can be achieved in the stripping and absorption section using dry membranes corresponding to a k_m value of 10^{-3} m/s and external fiber radius of 200 μ m. For significant absorber intensification factor, fibers should have an external radius less than 400 μ m and membrane mass transfer coefficient should not be less than $5 \cdot 10^{-4}$ m.s⁻¹. HFMC implementation for high temperature stripping is promising providing that membranes resistant to high temperature (i.e 120°C) and equally resistant to wetting are available. Due to important water transfer in both absorber and desorber, in addition to wetting of porous membranes by liquid breakthrough, a new possible limiting phenomenon for HFMC technology is wetting by capillary condensation. Even though net solvent losses in the membrane contactor are smaller than those calculated for packed columns, a scrubbing section after the HFMC is still required for solvent recovery in order to meet solvent concentration standard in the CO₂ depleted gas stream. This issue represents an opportunity for the membrane contactor technology based on dense-film MEA selective composite membrane.

Keywords: Carbon dioxide capture, adiabatic modeling, Hollow fiber membrane contactor, chemical absorption, solvent regeneration, intensification

Highlights :

- Important temperature variation as well as significant water transmembrane fluxes occurs in both absorber and desorber.
- Promising intensification factor for both absorption and desorption are obtained
- Fiber radius and membrane mass transfer coefficient are key with respect to process intensification issues.
- Membrane wetting of porous membranes influences strongly the overall absorption and desorption performance.
- High temperature stripping using membrane contactor is a promising technology providing that membranes can resist high temperatures and wetting.
- Net solvent losses in the membrane contactor are smaller than those calculated for packed columns.

Nomenclature

Latin symbols

a	: Specific interfacial area ($\text{m}^2 \cdot \text{m}^{-3}$)
a_d	: Dry specific area ($\text{m}^2 \cdot \text{m}^{-3}$)
C	: Molar concentration ($\text{mol} \cdot \text{m}^{-3}$)
C_p	: Specific heat ($\text{J} \cdot \text{mol}^{-1} \text{K}^{-1}$)
d_h	: Hydraulic diameter (m)
D	: Diffusion coefficient ($\text{m}^2 \cdot \text{s}^{-1}$)
E	: Enhancement factor (dimensionless)
G	: Molar flux of gas phase ($\text{mol} \cdot \text{m}^{-2} \cdot \text{s}^{-1}$)
Gz	: Graetz number (dimensionless)
h	: Heat transfer coefficient ($\text{W} \cdot \text{m}^{-2} \text{K}^{-1}$)
ΔH_{abs}	: Enthalpy of absorption ($\text{J} \cdot \text{mol}^{-1}$)
ΔH_{vap}	: Enthalpy of vaporization ($\text{J} \cdot \text{mol}^{-1}$) κ
K_{eq}	: Chemical equilibrium constant (molar scale)
\mathcal{K}	: Vapor liquid (VLE) equilibrium constant [--]
K_{koz}	: Kozeny constant (m^{-2})
k	: Mass-transfer coefficient ($\text{m} \cdot \text{s}^{-1}$)
k_{ov}	: Overall mass transfer coefficient ($\text{m} \cdot \text{s}^{-1}$)
L	: Molar flux of liquid phase ($\text{mol} \cdot \text{m}^{-2} \cdot \text{s}^{-1}$)
k_{M,CO_2}^{ref}	: Reference membrane transfer coefficient of CO_2 at 40°C and 1 bar ($\text{m} \cdot \text{s}^{-1}$)
D_{G,CO_2}^{ref}	: Reference diffusion coefficient of CO_2 at 40°C and 1 bar ($\text{m}^2 \cdot \text{s}^{-1}$)
N	: Molar flux ($\text{mol} \cdot \text{m}^{-2} \cdot \text{s}^{-1}$)
P	: Pressure (Pa)
q	: Heat flux ($\text{W} \cdot \text{m}^{-2}$)
r_e	: External fibre radius (m)
r_{CO_2}	: Reaction rate relative to CO_2 ($\text{mol} \cdot \text{m}^{-3} \cdot \text{s}^{-1}$)
R	: Gas constant ($\text{J} \cdot \text{mol}^{-1} \text{K}^{-1}$)
T	: Temperature (K)
U	: Overall heat transfer coefficient ($\text{W} \cdot \text{m}^{-2} \text{K}^{-1}$)
u	: Superficial fluid velocity ($\text{m} \cdot \text{s}^{-1}$)
v	: Interstitial fluid velocity ($\text{m} \cdot \text{s}^{-1}$)
Z	: Effective contactor length (m)

Greek symbols

α	: CO_2 solvent loading ($\text{mol}_{\text{CO}_2} \cdot \text{mol}_{\text{MEA}}^{-1}$)
δ	: Fiber thickness (m)
ϕ	: Packing fraction (dimensionless)
λ	: Thermal conductivity ($\text{W} \cdot \text{m}^{-1} \text{K}^{-1}$)
μ	: Viscosity ($\text{Pa} \cdot \text{s}^{-1}$)
ρ	: Density ($\text{kg} \cdot \text{m}^{-3}$)
He	: Henry constant (C_G/C_L) (-)

Subscripts

i	: Compound
G	: Relative to gas
L	: Relative to liquid
M	: Relative to the membrane

int : Internal surface of the fibres

ext : External surface of the fibres

1. Introduction

CO₂ capture from large sources attracts considerable attention as a key strategy to mitigate greenhouse gas emissions. Energy production and industrial sectors are responsible of about 60% of the global CO₂ emissions. Among the different possibilities, post-combustion carbon capture and storage (CCS) is particularly interesting because it offers retrofit possibilities. Among the different investigated capture processes, gas-liquid absorption using MEA chemical solvent in packed column is classically considered to be the best available technology and commonly taken as a reference (**Liang et al., 2015, Steeneveldt et al., 2006**). However, the following major challenges must be addressed to achieve the technical and economic targets:

- (i) Decrease of the energy requirement of the solvent regeneration step, through novel solvent or heat integration approaches
- (ii) Decrease of the size of the installation through process intensification.

Particularly, the treatment of large quantities of flue gases requires equipment of a large size. Hollow fiber membrane contactors (HFMC) are considered as one of the most promising strategies for the intensification of gas-liquid absorption processes, particularly for post combustion CO₂ capture by absorption in chemical solvents. The key concept of a membrane contactor is to make use of permeable membrane acting as a physical barrier between the gas and the liquid, allowing non-dispersive gas-liquid contact. Thus, membrane contactor permits to avoid liquid entrainment and flooding, which limit the operational range of packed columns. Moreover, membrane contactors present a special interest in offshore and zero gravity application (i.e low equipment weight, no gravity-driven flow). The supplementary mass transfer resistance, due to the membrane, is expected to be overbalanced by the high interfacial area (a) provided by the membrane, which can be 2 to 10 times higher than in packed column leading potentially to large intensification factors [**Wickramasinghe, 1991, Cussler, 1992, Feron and Jansen, 2002, , Klassenn et al., 2008**].

A major limitation to membrane contactor development is related to porous membrane wetting issues and chemical stability on long term tests. Wetting is strongly related to solvent properties (viscosity and interfacial tension), membrane pore size, contact angle and transmembrane pressure through Laplace equation [**Saffarini et al., 2013**]. One of the most relevant performance parameter for industry is the average CO₂ specific transferred flux, defined as the quantity of CO₂ transferred per unit-volume of contactor. In order to evaluate effectively the intensification potential of the technology compared to packed column, a value around $1 \text{ mol} \cdot \text{m}^{-3} \cdot \text{s}^{-1}$ has been recommended to be taken as the base-line performances (performing packing) [**Favre and Svendsen, 2012**].

The main target of employing membrane contactors for this application is to provide a significant reduction in equipment size compared to the reference packed columns technology. No significant improvement in the specific energy requirement can be expected as the latter is principally governed by the nature of the solvent (mainly heat of reaction, loading capacity and kinetics), and is independent of the technology used be it packed column or membrane contactor.

In an industrial MEA plant for CO₂ post-combustion capture, the inlet and outlet solvent loadings of the absorption unit play a key role for the mass transfer performances and the recommended values are approximately 0.25 and 0.45 for the inlet and outlet loading, respectively, in order to minimize the energy requirement of the regeneration unit [**Khaisri et al., 2011, Tobiesen et al., 2007**]. Generally, an industrial chemical absorption plant is characterized by nearly complete solvent conversion as well as a partially loaded solvent.

HFMC has been widely investigated both experimentally and theoretically and promising results have been reported in literature in terms of intensification potential at the laboratory scale and in pilot plant investigations (i.e. showing intensification factors ranging from 2 to 8). A literature review is given in (Cui and deMontigny, 2013, Hillal and Ismail 2015, Luis Van Gerven et al., 2012 and Albarracin Zaidiza et al., 2014). The laboratory scale is characterized by mild operating conditions, corresponding to lab-gases (e.g. no ashes), short-term operation (e.g. no absorbent degradation), low reagent concentrations and conversions, i.e. high liquid-to-gas flowrate ratio and unloaded liquid absorbents. The pilot plant test using membrane contactor was mostly performed at low MEA conversion and relatively low CO₂ capture ratio, some of them using partially loaded liquid absorbents. These conditions do not apply to industrial framework. The only available data under industrial relevant conditions correspond to that obtained in the CASTOR campaign at the Esbjerg pilot plant using packed column.

Regarding HFMC modelling studies, process models of various complexities have been developed considering, almost exclusively, isothermal conditions and neglecting water transfer. Under mild conditions of laboratory scale and pilot plant experiments, the isothermal models have been shown to correctly describe the experimental data in HFMC (Albarracin Zaidiza et al., 2015). However, under high solvent conversion and relatively high CO₂ solvent loading, typical of industrial conditions, the strongly exothermic and endothermic absorption and desorption operations respectively, are expected to lead to important temperature variation as well as significant solvent transmembrane fluxes (Neveux et al., 2013). The intensification potential of the technology needs to be estimated within industrial relevant operating conditions. Besides, temperature variation will influence physicochemical and thermodynamic properties, membrane-solvent interaction, such as contact angle or the pore shape as well as membrane structure stability. The transport of volatile component, such as water, through the membrane may lead to their condensation in the membrane due to local over-saturations and capillary effect (Albarracin Zaidiza et al., 2015). In order to fill this gap, an adiabatic 1D and 2D models have been developed and compared, in our previous work, for CO₂ absorption using MEA solution under industrial conditions. The results reveal the importance of thermal effect and the necessity of adiabatic model for rigorous prediction of the performance of the technology, under industrial relevant conditions (Albarracin Zaidiza et al., 2016). The isothermal model has been shown to lead to overestimation of the contactor absorption performance up to 50% compared to adiabatic multi-component model. The comparison of adiabatic 1D and 2D models predictions showed similar results in term of CO₂ and water transfer for the investigated system characteristics. The good performance of the 1D approach, using mixing-cup concentrations and temperatures, can be explained by the fact that, as the reaction film is very thin, the concentrations profile of the reactants and products in the liquid phase are almost flat. The radial heat transfer being rapid, the radial temperature profiles are also flat. Thus, adiabatic 1D approach have been shown to be adequate and sufficient for the prediction of HFMC for CO₂ absorption within industrial relevant conditions. However, slower reaction or physical absorption systems could potentially lead to significant radial gradients and to situations that necessitate the 2D approach.

The majority of HFMC for CCS using amine solution have focused on CO₂ absorption and very limited number of studies has addressed the potential of HFMC for the stripping step. The regeneration process is industrially performed using packed columns with a sweep gas generated by a partial evaporation of the liquid absorbent at high temperature (e.g. 120°C under 2 bar).

As for the absorption step, thermal effect is expected to be also significant for the highly endothermic regeneration step. Thus, adiabatic model needs to be used for good process performance prediction. Furthermore, thermal balances and heat transfer calculations are necessary to estimate the water condensation, which is essential for the functioning of the stripper. The major contributions of the energy

requirement of the stripping step are the latent heat of water vaporization needed for stripping steam production and the heat required to reverse the absorption reaction.

Using modelling techniques and/or experimental setups, solely the low temperature stripping (LTS) boosted by vacuum or by the use of non-condensable sweep gases, such as nitrogen, has been investigated (Yan *et al.*, 2009, Koonaphapdeelert *et al.*, 2009, Khaisiri *et al.*, 2009, Simoni *et al.*, 2011, Fang *et al.*, 2012, Wang *et al.* 2014, Naim *et al.*, 2014, Scholes *et al.*, 2016). This is attributed to the fact that choices for suitable membrane materials that can withstand high temperature i.e. around 120°C are limited. Indeed, membranes must be temperature resistant (e.g. chemical or physical change which leads to membrane wetting). Ceramic materials have been proposed in order to implement HFMC for CO₂ stripping at high temperatures where most polymeric membranes would fail to operate [Koonaphapdeelert *et al.*, 2009]. New high-temperature-resistant composite-membranes though expensive composed of poly[1-(trimethylsilyl)-1-propyne] (PTMSP), have also been suggested [Dibrov *et al.*, 2014].

On the other hand, to our knowledge, the stripping section using HFMC under industrial operating conditions has not been addressed in the literature. Even if significant material challenges exist, is high temperature stripping using membrane contactor, under relevant industrial conditions capable of reducing the size of the stripping and absorption units?

In this work, the absorption/desorption loop, functioning under industrial relevant conditions, is simulated using the 1D adiabatic model previously identified to be more adequate for the investigated system and operational domain.

The operating conditions of the absorption/desorption loop used for the simulations are those of the reference industrial MEA process, using packed column corresponding to CASTOR campaign at the Esbjerg pilot plant, operating at its energetic optimum.

The axial temperature profiles as well as transmembrane specific flux of CO₂, H₂O and MEA for both absorption and desorption are shown and discussed. The intensification potential of HFMC for both steps is evaluated and the key influencing parameters evidenced. The temperature changes in the contactor as well as solvents transfer will be discussed. Potential MEA and water losses in the absorption/desorption unit is evaluated and the results discussed. Finally, the main conclusions and recommendation regarding the intensification potential and limitation of HFMC for both absorption and desorption, under industrial relevant conditions are exposed.

2. Simulation framework

2.1. Design basis

Figure 1 shows a general flowsheet of CO₂ capture on coal power plant flue gas, in the framework of carbon capture and storage (CCS) strategy. Flue gas is first pretreated: denitrified by selective catalytic reduction of NO_x to N₂ then passes through electrostatic precipitator for removal of most particulate matter and finally desulphurize by SO₂ removal with direct contact with limestone slurry. The pretreated flue gas is then sent to CO₂ capture unit where CO₂ is captured and concentrated in order to minimize compression and transportation costs. Two main constraints have to be satisfied [Davidson and Metz, 2005]: CO₂ capture ratio and CO₂ purity should be both high enough, typically above 90%. CO₂ captured is then dried to meet the standards of water content. However, further post-treatment may be needed to fulfill the required standards for CO₂ transport and storage. Typical operating conditions and gas composition is also indicated in **Figure 1**.

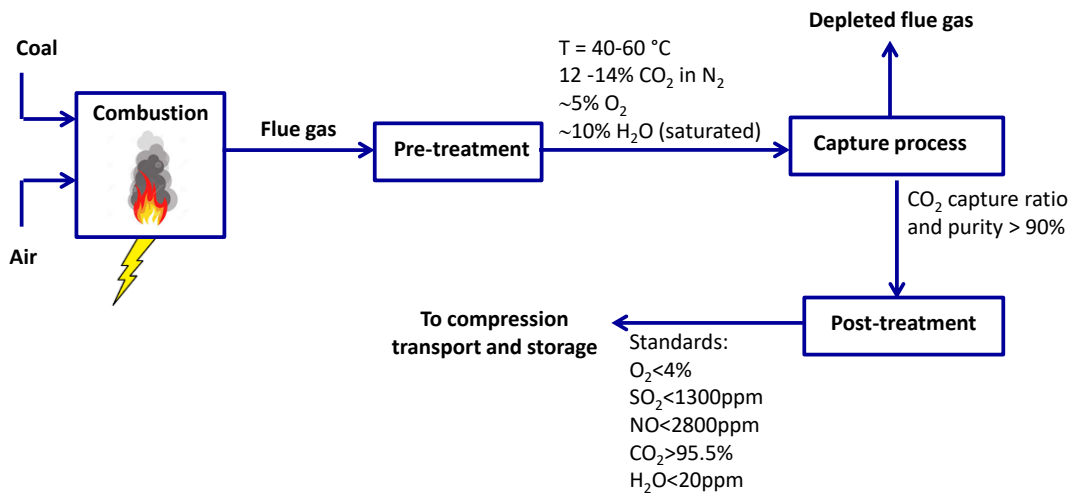


Figure 1: A general flowsheet of CO_2 capture on coal power plant flue gas, in the framework of carbon capture and storage (CCS) strategy.

In this work, the simulations have been achieved under industrial relevant conditions corresponding to those of CASTOR campaign at the Esbjerg pilot plant using packed column operating at its energetic optimum [Dugas et al., 2009]. The castor CO_2 capture pilot plant was built in the framework of a EU funded project, which started in 2004 and lasted 4 years. A pilot plant was built close to a coal fired power station operated by Dong in Denmark. It has been in operation since 2006, and was used for testing different solvent including MEA. The pilot plant capacity is approximately 1 ton CO_2 per hour [Kittel et al., 2009]. In the castor campaign experiments, the solvent is preloaded and the conversions of both, CO_2 and MEA at the contactor outlet are almost complete (a CO_2 capture ratio of ~ 0.90 and a CO_2 loading of rich solvent of $\alpha_{\text{rich}} \sim 0.48$). The purity of the recovered CO_2 is very high due to the selective reaction of CO_2 with amines. The absorber and desorber column height was of 17 m and 10 m respectively with a diameter of 1.1 m, filled with IMPT-50 packing. The regeneration factor was of $RF = 1 - (\alpha_{\text{lean}} / \alpha_{\text{rich}}) = 0.54$. While operating at its energetic optimum at reboiler pressure of 2 bars, the reboiler heat duty was of 3.75 GJ per ton of absorbed CO_2 .

The operating conditions (temperature, pressure, lean and rich solvent loading) are indicated in the flow sheet of absorption/desorption loop presented in **Figure 2**.

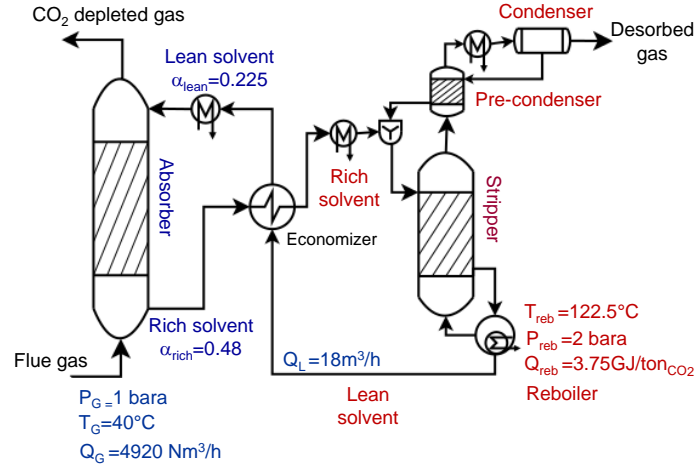


Figure 2 : Post-combustion CO_2 capture unit based on gas–liquid absorption using chemical solvent (MEA). Operating conditions of the CASTOR campaign from the Esbjerg pilot plant, - at the energetic optimum, regeneration factor $RF=1-(\alpha_{lean}/\alpha_{rich})=0.54$, CO_2 capture ratio of 0.90, $Z_{absorber}=17\text{m}$, $Z_{desorber}=10\text{m}$, column diameter $D=1.1\text{m}$, packing: IMPT 50 [Dugas et al., 2009]

The flue gas circulates counter currently to the solvent solution in an absorber where CO_2 is separated from the flue gas exiting the power plant by absorption in Amine solution. Almost pure CO_2 can be produced after drying. The rich loaded solvent is then heated in the economizer (heat exchanger) and sent to the tripping section to be regenerated by partial evaporation in a reboiler. The gas exiting the stripper is condensed and the condensate is sent back to the top of the stripper. The regenerated solvent (lean solvent) is then cooled in the economizer by the rich solvent and sent to the absorber in a close recycle loop.

2.2. Membrane and module characteristics

The membrane contactor consists of a bundle of cylindrical hollow fibres, made of hydrophobic microporous membranes. The contactor has an effective length, Z , an external radius, r_e , a fibre volume fraction, ϕ , and a relative thickness, δ/r_e . The geometric characteristics of the HFMC are calculated as shown in **Table 1**. For both absorption and desorption steps, the gas flows through the shell, and the liquid through the lumen in a countercurrent flow arrangement (**Figure 3**). The key membrane contactor characteristics related to intensification potential are mainly related to the material properties (membrane mass transfer coefficient), fiber geometry (diameter and thickness) and module (packing fraction, length) [Rode et al, 2012].

The membrane performance is characterized by components mass transfer coefficient through the membrane $k_{M,i}$. It depends on the fiber thickness, membrane porosity ϵ , and tortuosity τ , as well as on the pore-size distribution. The wide range of both, pore-sizes and pore-shapes, leads to a hardly reliable measure of the tortuosity and of the pore sizes. In this work, the membrane mass-transfer coefficient of component i is calculated considering CO_2 membrane mass-transfer coefficient as a reference, k_{M,CO_2}^{ref} . The reference conditions were set to 40°C and 100 kPa . The CO_2 membrane mass-transfer coefficient was fixed to typical values reported in literature (see **Table 2**), and not related to the fiber thickness and the material. Wetting phenomena are considered to affect all components in the same way. Accordingly, for multicomponent mass transfer through the microporous membrane, the mass transfer coefficient of the specie i was determined by Equation 1.

$$k_{M,i} = \frac{k_{M,CO_2}^{ref}}{D_{CO_2,G}^{ref}} D_{i,G} \quad (1)$$

In addition, due to wetting and capillary condensation that may occur along the membrane, CO₂ membrane mass transfer coefficient may vary over the contactor length. However, previous simulations under typical industrial conditions achieved by considering axial distribution of k_{M,CO_2} with 90% deviation from the mean value (i.e. equivalent k_{M,CO_2}) indicate that the use of an average equivalent mass-transfer coefficient appears to be adequate for the modelling of membrane contactor [Albarracin et al., 2016]. Thus, in the following, we assume constant equivalent membrane mass-transfer coefficient over the contactor length.

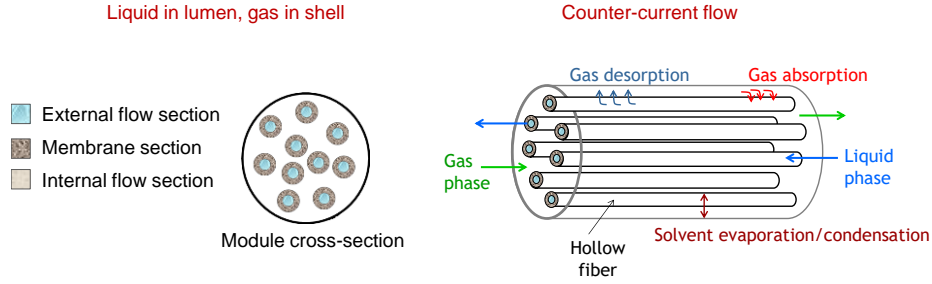


Figure 3: Pattern and flow section considered in the simulation.

Table 1: Expression of geometrical characteristics of the HFMC.

External and internal hydraulic diameter (m)	$d_{h-ext} = 2r_e \frac{1-\varphi}{\varphi}$, $d_{h-int} = 2r_e (1 - \delta/r_e)$
Internal and external specific interfacial area (-)	$a_{ext} = 2\varphi/r_e$, $a_{int} = 2\varphi(1 - \delta/r_e)/r_e$
Specific membrane area (-)	$a_M = \frac{2\varphi}{r_e} \frac{\delta/r_e}{\ln\left(\frac{1}{1 - \delta/r_e}\right)}$

Among commercially available microporous membranes, PTFE shows good resistance to wetting with acceptable k_m value in the range 10^{-4} - 10^{-3} m.s⁻¹. For simulation purposes the k_{M,CO_2} was varied within the range 10^{-5} - 10^{-2} ms⁻¹ to simulate dry and partially wetted porous membranes respectively, as indicated in **Table 2**. **Figure 4** shows the order of magnitude of membrane mass transfer coefficient for PCC using HFMC. When set, the fiber external radius was equal to 200 μm and the relative thickness equal to 0.2. The fiber packing fraction was set to 0.6, corresponding to industrial modules.

Table 2: Geometrical characteristics of the HFMC used in the simulation. The value between brackets corresponds to the base case.

External fibre radius (μm)	100-500 (200)
Relative fibre thickness= δ/re (-)	0.2
Packing fraction (-)	0.6
CO ₂ mass transfer coefficient in membrane, k_{M,CO_2}^{ref} (m s ⁻¹)	10^{-5} - 10^{-2} (10^{-3})

2.3. Reaction and system thermodynamics

The physicochemical properties of the gas and liquid were calculated using correlations available in literature showing excellent agreement with experimental data. The thermodynamic model proved to be physically consistent and relatively simple to implement and led to good predictions of thermodynamic properties. The reaction kinetics formulation taken from literature was adapted to be consistent with the thermodynamic model used in this work. Details can be found in our previous paper [Albarracin et al., 2016]. Since ionic species in solution are considered to be non-volatile, the phase equilibria are established for CO₂, MEA, H₂O and N₂. The chemical speciation of the aqueous MEA-CO₂ solutions was estimated using the equilibrium model of Astarita *et al.* [Astarita et al., 1993]. The termolecular reaction mechanism has been used to describe the reaction kinetics as it is suitable for partially loaded primary amines [Aboudheir et al., 2003]. A schematic representation of the reaction and thermodynamics of the system is shown in Figure 4.

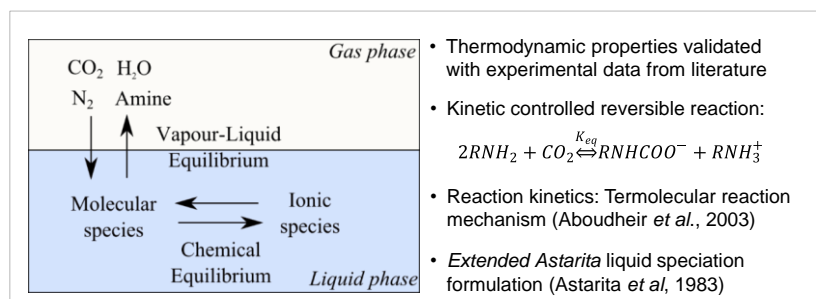


Figure 4: Schematic representation of the reaction and thermodynamics of the studied system.

2.4. Modeling

In this work, 1D adiabatic model has been used to simulate both absorption and desorption units. In this model, boundary layer theory was used to describe the gas and liquid-side mass and heat transfer [Beek, 1999]. Accordingly, mixing cup concentration and mixing cup temperatures were considered (Figure 5). Mass transfer is considered for three species ($i=CO_2, H_2O, MEA$). The illustrative reactive species ($i=CO_2$) diffuses from the gaseous phase to the gas-membrane interface, it then diffuses through the membrane pores, and is finally absorbed at the membrane-liquid interface by the liquid solution where it reacts. For desorption, CO₂ is released by the reverse reaction, diffuses in the liquid phase before being desorbed at the liquid-membrane interface, it then diffuses in the membrane pores and the gas phase. Local overall mass and heat transfer coefficients are computed using resistance in series approach in the three phases; liquid, membrane and gas. The local mass and heat transmembrane flux is expressed linearly as function of the local overall mass-transfer coefficients, specific membrane area and local driving force. The main model hypothesis, mostly based on general consensus found in other publications work, is summarized in Table 3. The mass, heat and momentum balance equations characterizing the system are given in Table 4. The membrane thermal conductivity was set to 0.15 W.m⁻¹ K⁻¹.

In reactive absorption and stripping operations, diffusion and reaction mechanism are coupled. A rate controlled reaction occurs in the liquid absorbent leading to mass transfer enhancement. In the investigated system, an enhancement factor expression for a second order reversible reaction is used to describe the chemical reaction in the liquid side diffusion boundary layer (**Decoursey, 1982; Veiland et al, 1982**). The mixing cup concentrations at the liquid phase were at chemical equilibrium whereas in the boundary layer, the reactions were kinetically controlled. In order to describe the diffusion in the boundary layer, the effective diffusivity methods for all compounds (molecules and ions) was used.

Given the high fiber length to internal diameter ratio, the flow in the lumen side can be considered as plug flow. Liquid and gas flow were considered to be laminar with fully developed velocity and temperature profiles. In the operating conditions considered in this work, these assumptions were shown to be valid (**Rode et al., 2012**). Furthermore, the liquid-side diffusion coefficient of each species is considered to be constant [**Chang and Rochelle, 1982**]. In laminar flow and for diluted species systems and low mass transfer rates, the mass and heat transfer processes are commonly treated by transfer analogies (Chilton –Colburn analogy) [**Beek, 1999, Skelland 1985**]. In laminar flow through a cylindrical pipe, the convective heat and mass-transfer coefficients can thus be estimated by integrating the Graetz equation for suitable boundary conditions [**Levêque, 1928**]. Details of mass and heat transfer coefficient calculation are given in **Appendix A**.

Table 3: Main 1D model hypothesis: Hydrodynamic, thermodynamic, reaction and mass and heat transfer.

Hydrodynamics	<ul style="list-style-type: none"> • Steady state • Laminar liquid and gas flow with fully developed velocity • Plug flow , i.e, non-uniform flow distribution due to random packing neglected
Thermodynamic	<ul style="list-style-type: none"> • Equilibrium at G-L interface according to Henry’s law • Ideal gas and Henry’s law used to represent the gas-liquid equilibrium
Reaction and mass transfer	<ul style="list-style-type: none"> • Rate controlled reversible reaction • Ionic products considered as one complex with a single apparent diffusion coefficient • Liquid-side diffusion coefficient of each species is considered to be constant • Fick diffusion through the membrane, no convective contribution.
Heat transfer	<ul style="list-style-type: none"> • Condensation and evaporation of water occurs only at the liquid-membrane interface • Adiabatic behavior thus neglecting heat losses • Thermal conduction in the membrane

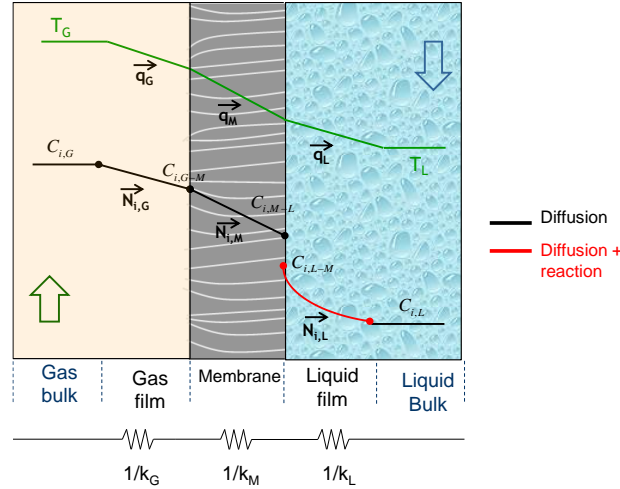


Figure 5: Schematic representation of mass transfer according to boundary layer theory – illustration of resistance in series approach.

The stripping section is described by the same equations as the absorber model. Considering the high temperature of the stripping unit, the chemical reactions are assumed to be at chemical equilibrium. Contrary to the absorption step, where the section is solely constituted by the gas-liquid contactor, the stripping unit is constituted by a whole of unit operations including mixers, heat exchanger, a pre-condenser and a condenser as shown in **Figure 2**. The pre-condenser consists in an extra packed bed placed at the top of the column and was simulated as a one-stage unit-operation at thermodynamic equilibrium by using a mixer followed by a flash separator.

The ordinary differential equation system of the HFMC as well as the stripping auxiliary operations is modeled and solved using Matlab[®] code.

Table 4: Mass, heat and momentum balance equations characterizing the 1D modeling approach.

One-dimensional modelling approach	
Mass balance	Gas : $\frac{d}{dz}L_i = -N_i$ where : $L_i = \bar{u}_L \bar{C}_{i,L}$ (2)
	Liquid : $\frac{d}{dz}G_i = -N_i$ where : $G_i = \bar{u}_G \bar{C}_{i,G}$ (3)
	With local mass flux computed using resistance in series approach :
	$N_i = a_M k_{i,ov} (\bar{C}_{i,G} - \bar{C}_{i,L}^*)$ (4)
	$\frac{1}{a_M k_{i,ov}} = \frac{1}{a_{ext} k_{i,G}} + \frac{1}{a_M k_{i,M}} + \frac{H e_i}{a_{int} E_i k_{i,L}}$ (5)
Energy balance	Gas : $\frac{d \bar{T}_G}{dz} = -\frac{q}{c_{pG} \sum_i G_i}$ (6)
	Liquid: $\frac{d \bar{T}_L}{dz} = -\frac{q + \sum_i N_i \Delta H_{abs/vap}}{c_{pL} \sum_i L_i}$ (7)
	With local heat flux computed using resistance in series approach :
	$q = a_M U (\bar{T}_G - \bar{T}_L)$ (8)

$$\frac{1}{a_M U} = \frac{1}{a_{ext} h_G} + \frac{1}{a_M h_M} + \frac{1}{a_{int} h_{i,L}} \quad (9)$$

	Fluid in lumen (Hagen Poiseuille)	$\frac{d P_{int}}{dz} = -\frac{8\mu_{int}\bar{v}_{f,int}}{r_i^2}$	(10)
Momentum balance	Fluid in shell (Happel, 1969):	$\frac{d P_{ext}}{dz} = -\mu_{ext}\bar{v}_{f,ext}\mathbf{K}_{koz}$	(11)
	With:	$\mathbf{K}_{koz} = \frac{8\varphi}{[2\ln(1/\varphi) - 3 + 4\varphi - \varphi^2]r_e^2}$	

\bar{T} and \bar{C} denote the mixing-cup temperature and concentration respectively at a given axial position, z.

\bar{u}_f stands for the mean superficial velocity at a given axial position z.

\bar{v}_f stands for the mean interstitial velocity at a given axial position z.

* Denotes equilibrium conditions

3. Simulations results

3.1. Models validation

Due to the current lack of experimental data, the membrane contactor model could not be validated for industrial operating conditions. The transfer model was therefore verified by the modelling, simulation and validation of the CO₂ capture process using packed column under the same conditions than those of CASTOR campaign at the Esbjerg pilot plant. Indeed, by setting the adequate mass-transfer correlations and by removing the terms related to the membrane, the 1D approach described in this work has been adapted to model packed columns. Details of packed column modeling are given **Appendix B**.

The tests performed in the CASTOR campaign at the Esbjerg pilot plant were then simulated and the comparison between simulations and experiments are illustrated in **Figure 6** for both absorber and desorber.

Good agreements between experimental data and model prediction were obtained for the two process steps, i.e. absorption and stripping. The absorption column performances are predicted within an uncertainty lower than 5%, thus demonstrating the quality of the kinetic and thermodynamic approach used in this work. The stripper step performances are predicted within an uncertainty of about 15% which is higher than that of the absorber step. The regeneration step carries many sources of uncertainties associated with experimental uncertainties, unknown reaction kinetics and few experimental data of liquid-vapor equilibria at high temperatures [**Neveux et al., 2013, Harbou et al., 2014, Tobiesen et al., 2008, Harbou et al., 2014**].

The model predicts correctly the temperature profiles, which evidences the non-isothermal behavior of the absorption and desorption units. Analogous temperature trends, at industrial operating conditions, have been reported in literature [**Dugas et al., 2009, Tobiesen et al., 2007, Neveux et al., 2013**]. Similar temperature profiles can be expected to occur in membrane contactors with similar boundary conditions. The average CO₂ specific transferred flux, defined as the quantity of CO₂ transferred per unit-volume of contactor, is one of the most relevant parameters for industry. Using packed column the average transferred CO₂ was 0.45 and 0.418 mole of CO₂ per unit contactor volume, for the absorption and the desorption unit respectively. For more performing packing type, a higher value is obtained around 1 mol.

$\text{m}^{-3}.\text{s}^{-1}$, value which is recommended to be taken as the base-line performances when comparing membrane contactor modules and the reference packed column technology performances (Favre and Svendsen, 2012).

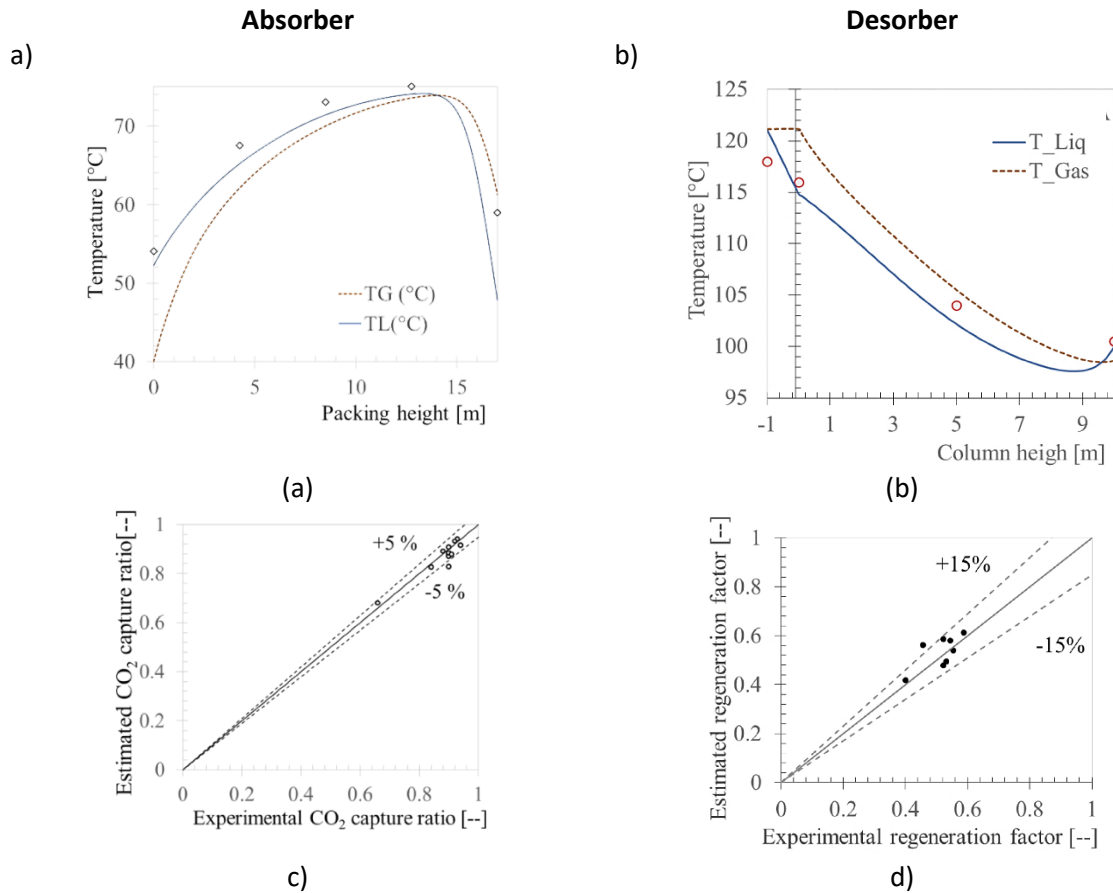


Figure 6: Simulation results of the packed column model. Solid and dotted lines: model predictions. Dots: experimental data. a) and b) temperature profile of the absorber and stripper respectively. c) and d)) parity plot of CO₂ capture ratio and regeneration factor for the absorber and desorber respectively. $Z_{\text{absorber}}=17\text{m}$, $Z_{\text{desorber}}=10\text{m}$. Data from the CASTOR campaign at the Esbjerg pilot plant [Dugas et al., 2009].

1.1. Axial profiles of fluids temperature and water transmembrane fluxes

In post-combustion CO₂ capture framework, high flue gas flow rates are to be treated at low pressure (atmospheric). Thus, to ensure a good distribution of gas flow rates in the membrane contactors, a pressure drop of 5% (e.g. 50 mbar) of the inlet pressure is recommended. Besides, post-combustion flue gases impose low gas pressure drops, in order to prevent a potential energy penalty in compression, but not so low as to jeopardize the gas distribution in the contactor. In the simulations, as for the reference process using packed column, the pressure drop in the absorption unit is set at 50 mbar. For the stripping unit, pressure drops of less than 300 mbar were aimed. The membrane contactor length was therefore varied to achieve the inlet and outlet solvent loading of the energetic optimum of the Esbjerg pilot plant. The HFMC length for the absorption and desorption was 0.32m and 0.5 m respectively. With such short

contactors and a large flux of flue gas to treat, the number of modules set in parallel will be important; hence, distribution and collection issues, typical of parallel circuits, should be studied rigorously.

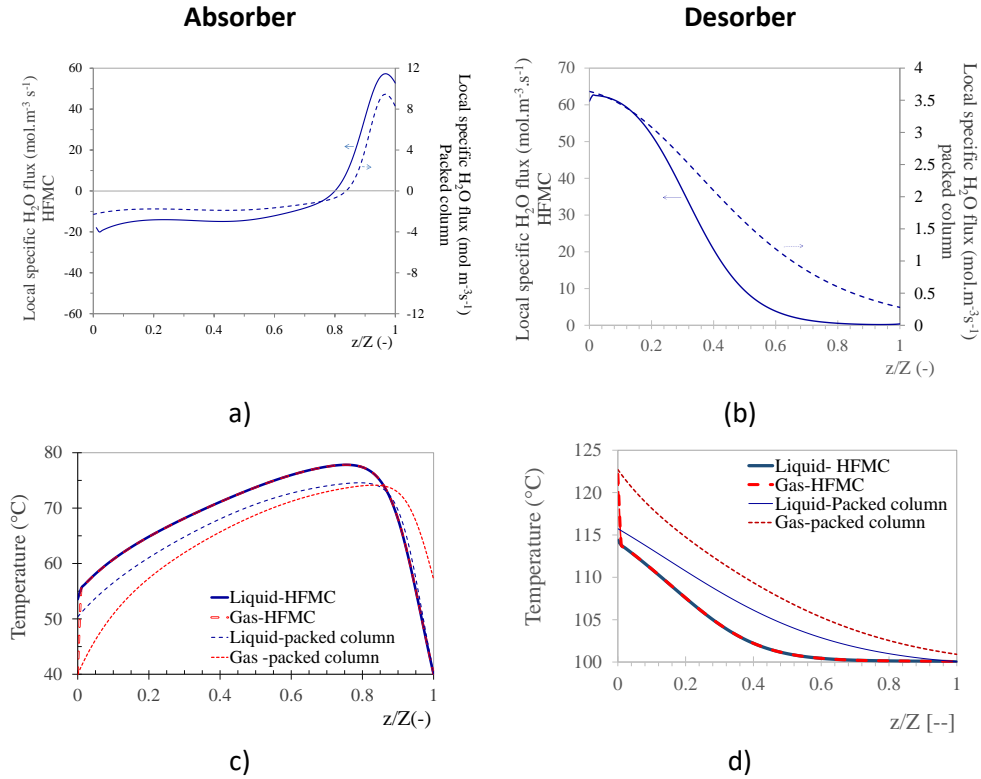


Figure 7: Axial profiles of transmembrane water flux and liquid temperature. $k_{m,CO_2} = 10^{-3} \text{ ms}^{-1}$. Simulation results of both technologies are shown: HFMC (solid line) and packed column (dashed line). a) and b) water interfacial fluxes in the absorber and desorber respectively c) and d) fluid temperature in the absorber and desorber respectively. Gas and liquid temperature profiles in the membrane contactor are superimposed.

The simulation results using HFMC were compared to those using packed columns. Both absorber and desorber simulations are systematically shown. Temperature profiles as well as H₂O local specific flux are shown in **Figure 7**. In addition, MEA and CO₂ local specific flux are shown in **Figure 8 and 9** respectively. First, it can be observed that similar temperature profile trends are obtained in packed column and HFMC even though over a much longer column. However, the local specific flux values corresponding to the latter are nearly one order of magnitude lower, due to the intensification provided by the HFMC. This highlights the homothety between both technologies concerning the axial profiles of temperature and interfacial fluxes.

In **Figures 7, 8 and 9**, positive values of local flux indicate the absorption or condensation of the component at the membrane-liquid interface; conversely, negative values indicate desorption or evaporation.

Figure 7a indicates that water flux reversal occurs, thus both water evaporation and condensation occurs in the absorber. Accordingly, as shown in **Figure 7c**, temperature profile in the absorber passes through a maximum temperature of approximately 80°C for the HFMC, near the liquid inlet ($z/Z=1$). The corresponding maximum temperature variation was around 35°C. Compared to packed column, this temperature peak was slightly higher in the HFMC.

However, as shown in **Figure 7b**, no water evaporation takes place inside the desorber indicating that the latent heat of water condensation is converted to CO₂ heat of desorption and to liquid sensible heat. The energy supplied to the reboiler leading to a partial evaporation of the liquid, is released over the column by water condensation. Thus, contrary to the absorber, the liquid temperature variation of the stripper is monotone and increases continually from the liquid inlet, with a total temperature variation of 15°C in the HFMC, as observed in **Figures 7d**.

In addition, it can be seen that temperature profiles of the gas and liquid in the HFMC are very close due to the excellent heat transfer [Albarracin et al., 2015], by difference with the packed column technology. In the absorber, the outlet gas and liquid temperatures are respectively higher and lower for the packed column. In the desorber, gas and liquid temperature are higher for the packed column. As it will be shown in the following these differences between both technologies will impact H₂O and MEA losses.

Moreover, important amount of water, about 60 mol. m⁻³s⁻¹ condenses at the vapor inlet section (z/Z = 0) of the desorber. Approximately the same amount condenses at the gas outlet section (z/Z = 1) of the absorber. Consequently, the high water condensation in a small part of the contactor may increase the likeliness of membrane wetting, being porous or composite, through capillary condensation.

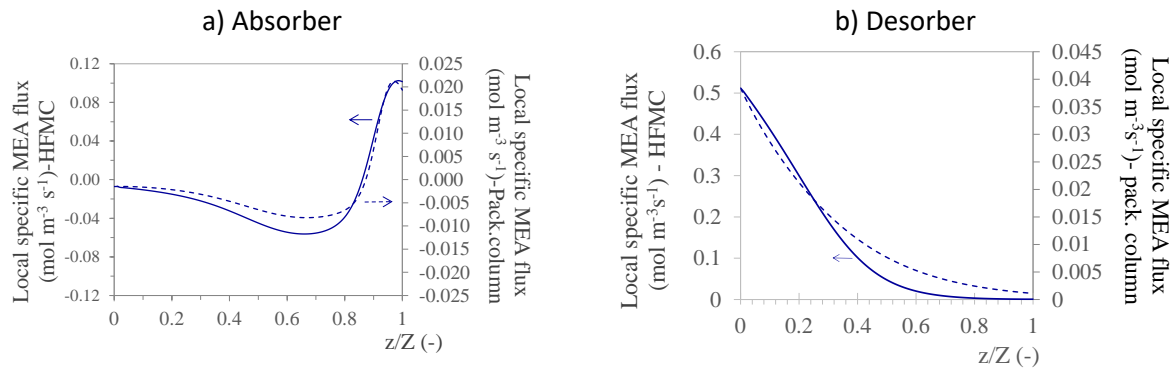


Figure 8: Axial profiles of the specific transmembrane fluxes of MEA, simulations of both technologies are shown: HFMC (solid line) and packed column (dashed line). (a) in the absorber (b) in the desorber.

Figures 8a and 8b show the axial profiles of the specific transmembrane fluxes of MEA in the absorber and desorber respectively. It can be seen that MEA vapor flux reversal occurs indicating that both MEA evaporation and condensation occurs in the absorber whereas in the stripper only MEA condensation occurs. The specific MEA flux is very low compared to that of CO₂ (**Figure 9**) by about two orders of magnitude.

Figure 9 shows the axial profiles of the specific trans-membrane fluxes of CO₂ for both absorption and stripping units. The absorbed specific flux of CO₂ passes through a maximum value of close to half-way along the length of the fiber as shown in **Figure 10a**. While, in the stripper (**Figure 10b**), the profile is monotone with almost no CO₂ transmembrane flux for membrane contactor lengths higher than 0.5 m. This means that the stripper reaches the thermodynamic equilibrium and the increase in the membrane length does not improve the separation performances, thus the stripper does operate near the thermodynamic equilibrium.

a) Absorber

b) Desorber

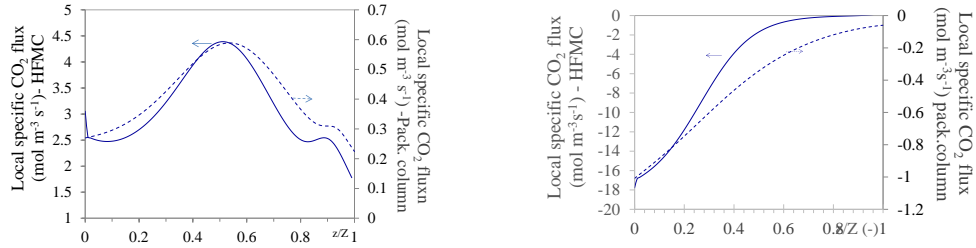


Figure 9: Axial profiles of CO₂ transmembrane specific flux estimated from adiabatic 1D modelling approach, simulations of both technologies are shown: HFMC (solid line) and packed column (dashed line). a) absorber b) desorber.

Since the local specific transmembrane molar flux of water can be more than 10 times higher than that of CO₂, the condensate is mainly composed by water. The transfer of water across the membrane is crucial because membrane wetting is likely to occur as both wetting conditions i.e. liquid breakthrough and vapour condensation may be locally surpassed. As condensable vapours pass through the membrane pores, it is likely for these vapours to condense within the membrane structure [Klaassen et al., 2005]. Membranes which are composed of a microporous support and a dense film, known as composite membranes, might prevent membrane wetting, due to the dense thin film on the liquid-side of the membrane which avoids the liquid breakthrough. However, capillary and film condensation may still occur. Consequently, experiments on long term in non-isothermal conditions, focusing on water transfer through hollow fibers membrane contactors need to be performed, in order to determine the influence of the phenomena mentioned here over.

3.3. Intensification potential of HFMC for the absorption and desorption units.

Using packed column under Castor Campaign conditions, the average absorbed and desorbed flux was of 0.45 and 0.42 mole of CO₂ per unit volume of the contactor (Table 5). However, in order to estimate the intensification factor, we consider in the following, the recommended base-line performance (value around 1 mol. m⁻³.s⁻¹ [Favre and Svendsen, 2012]). For an external fiber radius of 200 μm and km of 10⁻³ m.s⁻¹, a specific CO₂ absorbed flux of about 4.18 mol.m⁻³.s⁻¹ can be achieved using HFMC (see Table 5), corresponding to an intensification factor of about 3 and 4 of the absorber and stripper respectively.

Table 5: Predicted specific CO₂ transmembrane flux in both absorber and desorber – predicted fluxes in packed column are also shown for sake of comparison. External fiber radius 200 μm, relative fiber thickness= 0.2, packing fraction of 0.6 and k_{m, CO2} of 10⁻³ m.s⁻¹. Values between brackets correspond to Esbjerg pilot plant taken as a reference.

		CO ₂ Average specific transmembrane flux (mol. m ³ .s ⁻¹)		Intensification factor	
		K _{m,CO2} =10 ⁻³ m/s	K _{m,CO2} =10 ⁻³ m/s	K _{m,CO2} =10 ⁻³ m/s	K _{m,CO2} =10 ⁻⁴ m/s
Membrane contactor	Absorber	+3.13	3 (7)	1 (2)	
	Desorber	-4.18	4 (10)	1 (2)	
Packed column	Absorber	+0.45	-	-	

(castor Campaign)	Desorber	- 0.42	-	-
--------------------	----------	--------	---	---

In the absorber, the variation of the average CO₂ specific absorbed flux with CO₂ mass transfer coefficient of the membrane (k_M) for three external fiber radiuses is illustrated in **Figure 10**. The simulations indicate that in order to have a significant intensification factor, fibers should have an external radius less than 400 μm and membrane mass transfer coefficient must not be less than $5 \cdot 10^{-4} \text{ m} \cdot \text{s}^{-1}$. These results show the primary role of fiber radius and membrane mass transfer coefficient with respect to process intensification issues. The simulations indicate that a variation of one order of magnitude in the value of k_M , i.e. from 10^{-3} to $10^{-4} \text{ m} \cdot \text{s}^{-1}$, decrease significantly the intensification potential of the HFMC (See **Table 5** and **Figure 10**). In this sense, it must be pointed out that membrane wetting decreases dramatically the membrane mass transfer coefficient and thus the intensification potential of the technology.

To date, only polymers can fulfil the k_m requirement for significant process intensification (**Hussain and Koros 2007, Rode et al., 2012**). Due to its long term chemical stability and resistance to wetting in contact with amine solutions, PTFE appears to be one of the best performing materials (**Falk-Pedersen, 2008**). Regarding fiber radius, the results highlight the key role that is played by material constraints in the preparation of small-diameter fibers.

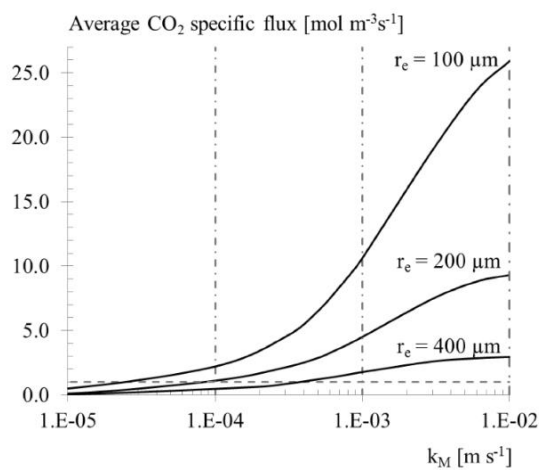


Figure 10: Variation of the average CO₂ specific absorbed flux with the mass transfer coefficient of the membrane for three external fibre radiuses. $k_M = 10^{-3} \text{ m} \cdot \text{s}^{-1}$. Relative thickness (δ/r_e) of 0.2.

3.4. Solvent losses estimation in both HFMC and packed column technologies

The loss of solvent in both absorption and desorption is important to consider in terms of operating costs and contactor performance, especially for long periods of operation.

H₂O and MEA losses are given in **Table 6** and expressed in ton and kg per ton of CO₂ captured respectively. In the stripping section, the solvent losses in the contactor and solvent recovery in the pre-condenser and condenser have been taken into account in the evaluation of the net solvent loss. The net losses correspond to the amount of solvent required to supply the process in steady state. Generally, it can be seen that solvent losses are significantly higher in the absorber than in the desorber.

The net losses in the membrane contactor are smaller than those calculated for packed columns. This is due to the excellent heat transfer in the HFMC resulting in closer liquid and gas temperatures. Consequently, in the packed column, higher gas outlet temperature in the absorber and higher gas and

liquid temperatures in the desorber are observed. This results in higher MEA and water vapour concentrations in the packed column, thus leading to increased solvent losses.

For illustration purposes, considering solely the absorption operation unit using HFMC, the total solvent losses would be of about 0.5 ton H₂O and 4.6 kg of MEA per ton of CO₂ captured. For a model coal power plant of 500 MW including carbon capture, these outputs would correspond to losses of around 5000 tons of water and 50 tons of MEA per day. In the absorption section, the predicted MEA concentrations in the outlet gas are 1.4 g/Nm³, value far above the upper limit for the design of a post-combustion CO₂ capture plant (i.e. 12 mg/Nm³ for MEA) [Khakharia *et al.*, 2013]. Therefore, in practical terms, a scrubbing section after the HFMC is required for solvent recovery. This issue represents an opportunity for the membrane contactor technology based on dense-film MEA selective composite membrane.

It is worth to mention that the emissions correspond to the total amount of solvent that would be present in the gas phase, whether in vapour state or as aerosol or fog. No general conclusions can be drawn since solvent emissions (mist and vapour) for flue gases are site-specific as well as specific to the conditions in which the tests are performed. Further analysis of solvent emissions modelling is out of the scope of this paper. Details of solvent emissions in the Esbjerg pilot plant are given in (Mertens *et al.*, 2013) and (Mertens *et al.*, 2014).

Table 6: Results synthesis – intensification factor and solvent losses, $k_{M, CO_2}=10^{-3}m/s$, $r_e=200 \mu m$.

		Net losses	
		H ₂ O (ton. ton _{CO₂} ⁻¹)	MEA (kg. ton _{CO₂} ⁻¹)
Membrane contactor	Absorber	0.50	4.60
	desorber	0.014	~ 0
Packed column (Castor)	Absorber	0.55	7.20
	Desober	0.024	0.305

3.5. Liquid in-lumen versus Liquid-in shell configurations

In the simulations, liquid in-lumen configuration has been considered. The influence of the liquid *in-shell* flow mode, with and without mixing points, on the contactor performance is investigated under industrial operating conditions. The results are shown in **Appendix C**.

In order to choose the adequate flow configuration for PCC process by means of HFMC, the process design engineer must consider the following aspects:

- The interfacial area per unit of contactor volume of the outer face of the fibers is higher than that of the inner face, as illustrated in **Figure C3** (See Appendix)
- CO₂ absorbed flux increase by a factor of 27% when switching from liquid in-lumen to liquid in-shell flow configuration. In addition, the use of shell mixing point could enhance the performance by a factor of 30% (See **Figure C2**).
- The pressure drop per unit of contactor length is higher in the shell, for fiber packing fractions of industrial interest, i.e. around 0.6, as illustrated in **Figure C**.
- The flow *in-shell* is subject to canalization issues (channeling and dead zones), particularly at high packing densities which increase the mass-transfer resistance. Moreover, the random nature of the packing as well as the non-uniform distribution of the fiber external radius lead

to non-uniform velocity distributions [Wickramasinghe et al., 1992, Bao et al., 1999, Wu and Chen, 2000]

- If the membrane is asymmetric, the face having the smaller pore size must be in contact with liquid to prevent liquid breakthrough.

4. Concluding remarks and outlook

In this work, the intensification potential of hollow fiber membrane contactors (HFMC) for CO₂ capture by chemical absorption using amine solution have been evaluated by simulation, for both absorption and desorption steps.

Regarding modeling and axial temperature and transmembrane fluxes, the main following conclusions can be derived:

- (i) The simulations under industrial conditions revealed the homothety between the packed column and the membrane contactor concerning the spatial profiles of temperature and interfacial fluxes.
- (ii) The strongly exothermic and endothermic absorption and desorption operations respectively, lead to important temperature variation as well as significant solvent transmembrane fluxes. Adiabatic models are thus required for realistic prediction of HFMC technology under relevant industrial condition
- (iii) The excellent heat transfer through the membrane contactor through the membrane together with the high water condensation in a small part of the contactor increases the likeliness of membrane wetting, being porous or composite, through capillary condensation.

Regarding the intensification potential of the technology, the following conclusions can be given:

- Compared to packed column, a contactor volume reduction (i.e. intensification factor) of about 4 and 3 can be achieved in the stripping and absorption section using dry membranes corresponding to a k_m value of 10^{-3} m/s
- Fiber radius and membrane mass transfer coefficient are key with respect to process intensification issues.
- Membrane wetting of porous membranes influences strongly the overall absorption and desorption performance.
- HFMC implementation for high temperature stripping is a promising technology providing that membranes can resist high temperatures and are equally resistant to wetting. Inorganic and composite membranes currently represent interesting theoretical candidates.
- Under industrial conditions, simulations of the absorption step showed that fiber with an external radius of less than 400 μ m and membrane mass transfer coefficient of more than $5 \cdot 10^{-4}$ m/s are necessary to obtain significant intensification factors.

Regarding solvent losses by evaporation, it can be concluded:

- (i) Net solvent losses in the membrane contactor are smaller than those calculated for packed columns. Still a scrubbing section after the HFMC is required for MEA recovery in order to meet concentration standard in the CO₂ depleted gas stream
- (ii) Dense-film composite membrane, being selective to the MEA, would reduce the amine vapour outflow.

Finally, the following perspectives and general comments can be proposed:

- (i) The 1D approach, using mixed-cup concentration and temperature proved to be correct in the investigated domain. However, slower reaction or physical absorption systems could potentially lead to significant radial gradients and to situations that necessitate the 2D approach.
- (i) Fundamental understanding of the wetting mechanisms under industrially relevant conditions would be helpful in order to develop reliable and still simple wetting models that could be implemented in the reactor model.
- (ii) For the HFMC to reach the industrial maturity and competitiveness with packed columns, there is a need for proven feasibility under industrial conditions, long term stability studies, reliable prediction of membrane wetting, integration in process flowsheeting and analysis of economic viability.
- (iii) While HFMC showed promising intensification factors and size reduction possibilities, the technology doesn't impact the energy requirement of the stripping step given that packed columns function industrially already at thermodynamic equilibrium thereby minimizing energy requirement.
- (iv) Selective dense composite membrane should be further investigated as an interesting option to limit both membrane wetting and solvent losses.

Appendices

Appendix A: Mass and heat transfer coefficients calculation

Mass transfer coefficients

In laminar channel flow through HFMC, the concentration polarization is predominant [Yan et al., 2009]. Two mass transfer zones are observed when the residence time is sufficiently high: the entry zone, characterized by a developing concentration boundary layer and high mass transfer coefficients, and the developed boundary layer zone, characterized by low mass transfer coefficients. The boundary layer on both, the liquid and the gas side, were computed by integrating the Graetz equation for the suitable hydraulic diameter [Saffarini et al., 2013]. For given ranges of the Graetz number, the Sherwood number is estimated by:

$$Gz_F < 0.03 \quad Sh_F = 1.3Gz_F^{-1/3} \quad (A1)$$

$$Gz_F > 0.03 \quad Sh_F = 4.36 \quad (A2)$$

Where Gz_F and Sh_F are the Graetz number and is the Sherwood number respectively. They are defined as:

$$Gz_F = \frac{D_{j,F} z}{v_F d_h^2} \quad (A3)$$

$$Sh_F = \frac{k_F d_h}{D_{j,F}} \quad (A4)$$

It is worth noting that the computed Sherwood values and mass transfer coefficients are related to the mixing cup concentration at the axial coordinate z . The value of the limiting Sherwood number (i.e. 4.36), corresponds to a boundary condition of uniform mass flux.

Heat transfer coefficients

In cross-flow HFMC with laminar flow (Happel's hydrodynamics), the estimated and measured values of the Nusselt number were very similar to those of the Sherwood number [Hoff et al., 2004, Wang et al., 2005]. Such results indicate that the application of the Chilton-Colburn analogy is appropriate [Zhang et al., 2006]. This analogy was successfully used in similar transfer systems (e.g. Air humidification) [Keshavarz et al., 2008]. For these reasons, it was applied here to estimate the heat transfer coefficients of both, the liquid and the gas phases. The heat transfer coefficient of the membrane was computed using the isostress or series model, as recommended by [Boucif et al., 2008]:

$$h_M = \frac{1}{\delta} \left[\frac{(1-\varepsilon)}{\lambda_M} + \frac{\varepsilon}{\lambda_G} \right]^{-1} \quad (A5)$$

For heat transfer calculations, the membrane porosity was set to 0.5 and the membrane thermal conductivity to $0.15 \text{ W}\cdot\text{m}^{-1}\text{K}^{-1}$.

Appendix B: Packed Column Model Equations

Details of packed columns modelling are found in [Tobiesen et al., 2007], [Neveux et al., 2011], [Harbou et al., 2014]. The differential balance as well as the transfer correlations is shown in **Table B1**. In addition, the Sherwood number and the interfacial specific area correlations are included for the IMPT-50 packing used in the Esbjerg pilot plant. The model assumptions of this model are similar to those of HFMC modelling, except for those relative to the membrane and the gas-phase flow regime, i.e. turbulent flow.

Table B1: Model equations of CO_2 absorption using packed columns. Transfer coefficients for packing IMPT-50, taken from [Hanley and Chen].

Mass	Energy
------	--------

Transfer equations	Gas and liquid: $\frac{d}{dz}G_i = \frac{d}{dz}L_i = -N_i$	Gas: $\frac{d\overline{T}_G}{dz} = -\frac{a_I U(\overline{T}_G - \overline{T}_L)}{c_{pG} \sum_i \overline{u}_G \overline{C}_{i,G}}$
	With: $G_i = \overline{u}_G \overline{C}_{i,G} \quad L_i = \overline{u}_L \overline{C}_{i,L}$ $N_i = a_I k_{i,ov} (\overline{C}_{i,G} - \overline{C}_{i,L}^*)$ $\frac{1}{k_{i,ov}} = \frac{1}{k_{i,G}} + \frac{K_i^{VLE}}{E_i k_{i,L}}$	Liquid: $\frac{d\overline{T}_L}{dz} = -\frac{a_I U(\overline{T}_G - \overline{T}_L) + \sum_i N_i \Delta H_{abs/vap}}{c_{pL} \sum_i \overline{u}_L \overline{C}_{i,L}}$
Transfer coefficients	Dimensionless numbers: $Re_f = \frac{\rho_f u_f d_h}{\mu_f}; Sc_{i,f} = \frac{\mu_f}{\rho_f D_{i,f}}$ $Sh_{i,f} = \frac{k_{i,f} d_h}{D_{i,f}}; We_f = \frac{d_h \rho_f u_f^2}{\sigma_f}$ $Fr_f = \frac{u_f^2}{g d_h}$	Dimensionless numbers: $Pr_f = \frac{\mu_f c_{p,f}}{\lambda_f}$ $Nu_f = \frac{h_f d_h}{\lambda_f}$
	Gas: $Sh_{i,G} = 0.00473 Re_G Sc_{i,G}^{1/3}$	Chilton-Colburn analogy $Sh_{i,f} Sc_{i,f}^{-1/3} = Nu_f Pr_f^{-1/3}$
	Liquid: $Sh_{i,L} = Re_f Sc_{i,G}^{1/3}$	With: $d_h = \frac{4\epsilon}{a_d}$
		$\frac{a_I}{a_d} = 0.332 Re_G^{0.132} Re_L^{-0.102} We_L^{0.194} Fr_L^{-0.2} \left(\frac{\rho_G}{\rho_L}\right)^{-0.154} \left(\frac{\mu_G}{\mu_L}\right)^{0.195}$

Appendix C: Liquid *in-shell* flow Configuration

In this section, the influence of the liquid *in-shell* mode flow, with and without mixing points, on the contactor performance is studied under industrial operating conditions and using the 1D modelling approach detailed previously. The liquid *in-shell* and *in-lumen* flow modes are illustrated in **Figure C1**. In order to simulate the baffles in terms of mass-transfer, the liquid Graetz numbers are reset to their inlet value at every baffle location. By doing this, a perfect mixing in the shell at the corresponding baffle location is assumed. The average CO₂ absorbed flux per unit of contactor volume as a function of the external fiber radius is illustrated in **Figure C2**, for the two flow modes, i.e. liquid *in-lumen* and liquid *in-shell* with and without mixing points. The increase of the contactor performance by switching the operating mode from liquid *in-lumen* to *in-shell* can be appreciated. This improvement is due to the increase of the membrane area in contact with the liquid, as shown in **Figure C3** which for the simulated cases was of 25% with respect to the inner surface. The increase of the contactor performance obtained by the introduction of mixing points is of about 20%. This improvement is attributed to the enhancement of the reactant diffusion, i.e. CO₂ and MEA. Indeed, due to the MEA depletion imposed by the low liquid-to-gas flow rate ratio, there is a zone of the module in which the reaction between CO₂ and MEA is limited by the supply of reactant.

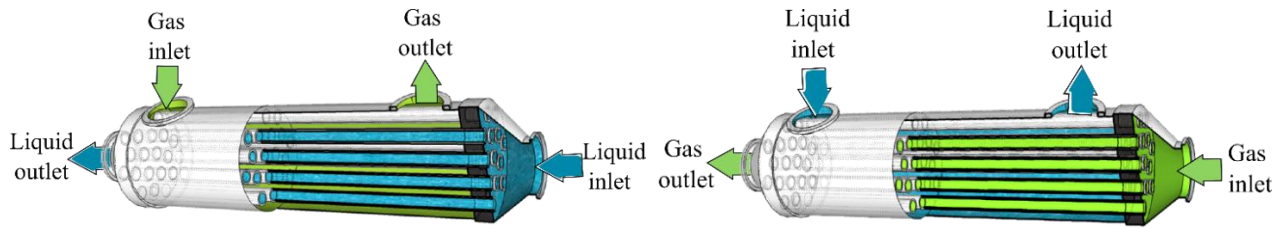


Figure C1 :Liquid in-lumen (left) and liquid in-shell (right) flow configurations of HFMC

Figure C4 compares the liquid pressure drop for liquid flowing in shelle and in lumen. The pressure drop for the shell side is significantly higher than that in lumen for high fiber packing fraction (typically above 50%) and low relative thicknesses. It should be mentioned that the liquid pressure drop changes from 15 to 90 mbar as a consequence of the flow mode. This is expected to be more significant when introducing the baffles. In addition to increasing the energy penalty by liquid pumping, the increase of the liquid pressure drop increases the probability of membrane wetting caused by liquid breakthrough.

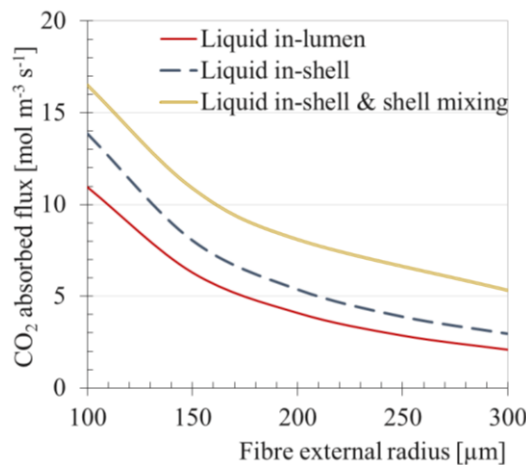


Figure C2: Variation of the average CO₂ absorbed flux per unit volume of contactor with the external fibre radius, for different flow configurations. $\delta/r_e=0.2$, $\phi = 0.6$, $k_{M,CO_2}^{eq} = 10^{-3}ms^{-1}$.

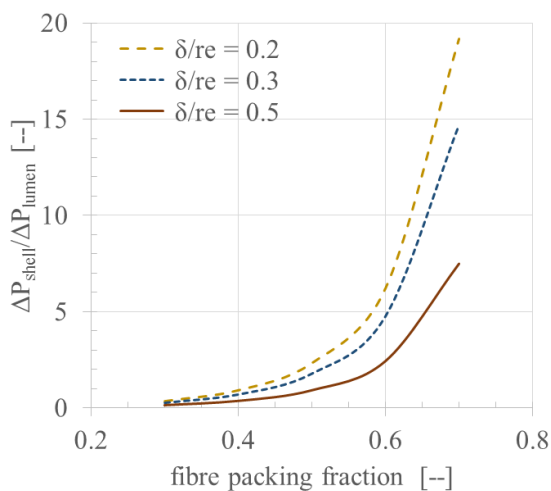


Figure C4: Shell and lumen pressure drop ratio as function of the fibre packing fraction.

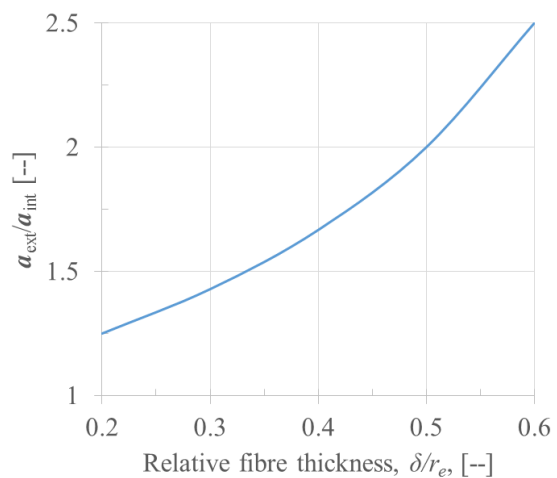


Figure C3: Ratio between the external and the internal specific interfacial area as function of the relative fibre thickness.

References

- Albarracin Zaidiza, D., Wilson S ;G, Belaissaoui, B., Rode S., Castel C., Roizard D., Favre E., Rigorous modelling of adiabatic multicomponent CO₂ post-combustion capture using hollow fibre membrane contactors, *Chemical Engineering Science*, Volume 145, 12 May 2016, Pages 45-58.
- Albarracin Zaidiza, D., Belaissaoui, B., Rode, S., Neveux, T., Makhloufi, C., Castel, C., Roizard, D., Favre, E., 2015. Adiabatic modelling of CO₂ capture by amine solvents using membrane contactors. *J. Membr. Sci.* 493, 106–119. doi:10.1016/j.memsci.2015.06.015, 2015
- Albarracin Zaidiza, D., Billaud, J., Belaissaoui, B., Rode, S., Roizard, D., Favre, E., 2014. Modeling of CO₂ post-combustion capture using membrane contactors, comparison between one- and two-dimensional approaches. *J. Membr. Sci.* 455, 64–74. doi:10.1016/j.memsci.2013.12.012
- Aboudheir, A., Tontiwachwuthikul, P., Chakma, A., Idem, R., 2003. Kinetics of the reactive absorption of carbon dioxide in high CO₂-loaded, concentrated aqueous monoethanolamine solutions. *Chem. Eng. Sci.* 58, 5195–5210. doi:10.1016/j.ces.2003.08.014
- Astarita, G., Savage, D.W., Bisio, A., 1983. *Gas treating with chemical solvents*. John Wiley.
- Beek, W.J., Muttzall, K.M.K., Heuven, J.W., 1999. *Transport phenomena*. Wiley.
- Bao L., Liu B., and Lipscomb G. G., “Entry mass transfer in axial flows through randomly packed fiber bundles,” *AIChE J.*, vol. 45, no. 11, pp. 2346–2356, Nov. 1999
- Beek W.J., Muttzall K.M.K., van Heuven J.M., *Transport Phenomena*, 2nd ed., John Wiley & Sons Ltd., London, 1999. [22] A.H.P. Skelland, *Diffusional Mass Transfer*, John Wiley & Sons Ltd., London, 1974.
- Boucif N., Favre E., and Roizard D., “capture in HFMM contactor with typical amine solutions: A numerical analysis,” *Chem. Eng. Sci.*, vol. 63, no. 22, pp. 5375–5385, Nov. 2008.
- Cui Z. and deMontigny D., “Part 7: A review of CO₂ capture using hollow fiber membrane contactors,” *Carbon Manag.*, vol. 4, no. 1, pp. 69–89, Feb. 2013.
- Chang, C.S., Rochelle, G.T., 1982. Mass transfer enhanced by equilibrium reactions. *Ind. Eng. Chem. Fundam.* 21, 379–385. doi:10.1021/i100008a011
- Davidson O., Metz B., *Special Report on Carbon Dioxide Capture and Storage*, International panel on climate Change, Geneva, Switzerland(2005) /http:// www.ipcc.chS.
- Dugas, R., Alix, P., Lemaire, E., Broutin, P., Rochelle, G., 2009. Absorber model for CO₂ capture by monoethanolamine - application to CASTOR pilot results, in: Gale, J., Herzog, H., Braitsch, J. (Eds.), *Greenhouse Gas Control Technologies 9*. Elsevier Science Bv, Amsterdam, pp. 103–107.
- Dibrov G. A., Volkov V. V., Vasilevsky V. P., Shutova A. A., Bazhenov S. D., Khotimsky V. S., van de Runstraat A., Goetheer E. L. V., and Volkov A. V., “Robust high-permeance PTMSP composite membranes for CO₂ membrane gas de-sorption at elevated temperatures and pressures,” *J. Membr. Sci.*, vol. 470, pp. 439–450, Nov. 2014.

Falk-Pedersen O., Dannström H., Separation of carbon dioxide from offshore gas turbine exhaust, *Energy Convers. Manage.* 38 (1997) 981–986.

Fang M., Wang Z., Yan S., Cen Q., and Luo Z., “CO₂ desorption from rich alkanolamine solution by using membrane vacuum regeneration technology,” *Int. J. Greenh. Gas Control*, vol. 9, pp. 507–521, Jul. 2012.

Favre E. and Svendsen H. F., “Membrane contactors for intensified post-combustion carbon dioxide capture by gas–liquid absorption processes,” *J. Membr. Sci.*, vol. 407–408, pp. 1–7, 2012.

Feron P.H.M., Jansen A.E., CO₂ separation with polyolefin membrane contactors and dedicated absorption liquids: performances and prospects, *Sep. Purif. Technol.* 27 (2002) 231–242.

Hanley B. and Chen C.-C., “New mass-transfer correlations for packed towers,” *AIChE J.*, vol. 58, no. 1, pp. 132–152, Jan. 2012.

Happel, J., 1959. Viscous flow relative to arrays of cylinders. *AIChE J.* 5, 174–177. doi:10.1002/aic.690050211

Harbou I. von, Imle M., and Hasse H., “Modeling and simulation of reactive absorption of CO₂ with MEA: Results for four different packings on two different scales,” *Chem. Eng. Sci.*, vol. 105, pp. 179–190, Feb. 2014.

Hilal N., Ismail A. F., and Wright C., *Membrane Fabrication*. CRC Press, 2015.

Hoff K. A., Juliussen O., Falk-Pedersen O., and Svendsen H. F., “Modeling and Experimental Study of Carbon Dioxide Absorption in Aqueous Alkanolamine Solutions Using a Membrane Contactor,” *Ind. Eng. Chem. Res.*, vol. 43, no. 16, pp. 4908–4921, 2004.

Husain S., Koros W.J., Mixed matrix hollow fiber membranes made with modified HSSZ-13 zeolite in polyetherimide polymer matrix for gas separation, *J. Membr. Sci.* 288 (2007)195–207.

Keshavarz P., Fathikalajahi J., and Ayatollahi S., “Analysis of CO₂ separation and simulation of a partially wetted hollow fiber membrane contactor,” *J. Hazard. Mater.*, vol. 152, no. 3, pp. 1237–1247, avril 2008.

Klaassen R., P.Feron. H. M., and Jansen A. E., “Membrane Contactors in Industrial Applications,” *Chem. Eng. Res. Des.*, vol. 83, no. 3, pp. 234–246, Mar. 2005.

Khakharia, P., Brachert, L., Mertens, J., Huizinga, A., Schallert, B., Schaber, K., Vlugt, T.J.H., Goetheer, E., 2013. Investigation of aerosol based emission of MEA due to sulphuric acid aerosol and soot in a Post Combustion CO₂ Capture process. *Int. J. Greenh. Gas Control* 19, 138–144. doi:10.1016/j.ijggc.2013.08.014

Khaisri S., de Montigny D., Tontiwachwuthikul P., Jiranatananon R., CO₂ stripping from monoethanolamine using a membrane contactor, *J. Membr. Sci.* 376 (2011) 110–118. [5] M. Simioni, S.E. entish, G.W. Stevens, Membrane stripping: desorption of carbon dioxide from alkali solvents, *J. Membr. ci.* 378 (2011) 18–27.

Koonaphapdeelert S., Wu Z., and Li K., “Carbon dioxide stripping in ceramic hollow fibre membrane contactors,” *Chem. Eng. Sci.*, vol. 64, no. 1, pp. 1–8, Jan. 2009.

Khaisri S., deMontigny D., Tontiwachwuthikul P., and Jiraratananon R., "CO₂ stripping from monoethanolamine using a membrane contactor," *J. Membr. Sci.*, vol. 376, no. 1–2, pp. 110–118, Jul. 2011.R.

Kittel J., Idem R., Gelowitz D., Tontiwachwuthikul, Parrain P. G. , Bonneau A. ,Corrosion in MEA units for CO₂ capture: pilot plant studies *Energy Procedia* 1 (2009) 791–797.

Liang Z., Rongwong W., Liu H., Fu K. et al., 2015. Recent progress and new developments in post-combustion carbon-capture technology with amine based solvents. *Int. J. Greenhouse Gas Control*, Special Issue commemorating the 10th year anniversary of the publication of the Intergovernmental Panel on Climate Change Special Report on CO₂ Capture and Storage 40, 26 – 54.

Lévêque J., Les lois de la transmission de chaleur par convection, *Ann. Mines Paris* (1928), vol. series 12.

Luis P., Van Gerven T., and Van der Bruggen B., "Recent developments in membrane-based technologies for CO₂ capture," *Prog. Energy Combust. Sci.*, vol. 38, no. 3, pp. 419–448, Jun. 2012.

Mertens, J., Brachert, L., Desagher, D., Thielens, M.L., Khakharia, P., Goetheer, E., Schaber, K., 2014. ELPI+ measurements of aerosol growth in an amine absorption column. *Int. J. Greenh. Gas Control* 23, 44–50. doi:10.1016/j.ijggc.2014.02.002

Mertens, J., Lepaumier, H., Desagher, D., Thielens, M.-L., 2013. Understanding ethanolamine (MEA) and ammonia emissions from amine based post combustion carbon capture: Lessons learned from field tests. *Int. J. Greenh. Gas Control* 13, 72–77. doi:10.1016/j.ijggc.2012.12.013

Naim, A. F. Ismail, N. B. Cheer, and M. S. Abdullah, "Polyvinylidene fluoride and polyetherimide hollow fiber membranes for CO₂ stripping in membrane contactor," *Chem. Eng. Res. Des.*, vol. 92, no. 7, pp. 1391–1398, Jul. 2014.

Neveux, T., Le Moullec, Y., Corriou, J.-P., Favre, E., 2013. Modeling CO₂ Capture in Amine Solvents: Prediction of Performance and Insights on Limiting Phenomena. *Ind. Eng. Chem. Res.* 52, 4266–4279. doi:10.1021/ie302768s

Qi Z., Cussler E.L., Hollow fiber gas membranes, *AIChE J.* 31 (9) (1992) 1548–1553. Fleur R. Klaassen, P. Feron, A. Jansen, Membrane contactor applications, *Desalination* 224 (2008) 81–87.

Rode, S., Nguyen, P.T., Roizard, D., Bounaceur, R., Castel, C., Favre, E., 2012. Evaluating the intensification potential of membrane contactors for gas absorption in a chemical solvent: A generic one-dimensional methodology and its application to CO₂ absorption in monoethanolamine. *J. Membr. Sci.* 389, 1–16. doi:10.1016/j.memsci.2011.09.042

Steenefeldt R., Berger B., Torp T.A., CO₂ capture and storage: closing the knowing-doing gap, *chem.eng.res.Des.* 84 (9) (2006) 739- 763.

Saffarini R. B., Mansoor B., Thomas R., and Arafat H. A., "Effect of temperature-dependent microstructure evolution on pore wetting in PTFE membranes under membrane distillation conditions," *J. Membr. Sci.*, vol. 429, pp. 282–294, Feb. 2013.

Scholes Colin A., Skentish andra E., Stevens Geoffrey W, deMontigny David, Asymmetric composite PDMS membrane contactors for desorption of CO₂ from monoethanolamine, *International Journal of Greenhouse Gas Control*, Volume 55, December 2016, Pages 195-201.

Simioni M., Kentish S.E. , G.W. Stevens, Membrane stripping: desorption of carbon dioxide from alkali solvents, *J. Membr. Sci.* 378 (2011) 18–27.

Tobiesen F. A., Juliussen O., and Svendsen H.F., “Experimental validation of a rigorous desorber model for post-combustion capture,” *Chem. Eng. Sci.*, vol. 63, no. 10, pp. 2641–2656, May 2008.

Tobiesen F.A., Svendsen H.F., Juliussen O., Experimental validation of a rigorous absorber model for CO₂ postcombustion capture, *AIChE J.* 53 (4) (2007) 846–865.

Wickramasinghe S.R., Semmens M.J., Cussler E.L., Better hollow fiber contactors, *J. Membr. Sci.* 62 (1991) 371–388.

Wickramasinghe S., M. Semmens, and E. Cussler, “Mass-Transfer in Various Hollow Fiber Geometries,” *J. Membr. Sci.*, vol. 69, no. 3, pp. 235–250, May 1992.

Weiland, R.H., Dingman, J.C., Cronin, D.B., Browning, G.J., 1998. Density and Viscosity of Some Partially Carbonated Aqueous Alkanolamine Solutions and Their Blends. *J. Chem. Eng. Data* 43, 378–382. doi:10.1021/je9702044.

Weiland, R.H., Rawal, M., Rice, R.G., 1982. Stripping of carbon dioxide from monoethanolamine solutions in a packed column. *AIChE J.* 28, 963–973. doi:10.1002/aic.690280611
DeCoursey, W.J., 1982. Enhancement factors for gas absorption with reversible reaction. *Chem. Eng. Sci.* 37, 1483–1489. doi:10.1016/0009-2509(82)80005-5

Wang Z., Fang M., Ma Q., Zhao Z., Wang T., and Luo Z., “Membrane Stripping Technology for CO₂ Desorption from CO₂-rich Absorbents with Low Energy Consumption,” *Energy Procedia*, vol. 63, pp. 765–772, 2014.

Wang R., Zhang H. Y., Feron P. H. M., and Liang D. T., “Influence of membrane wetting on CO₂ capture in microporous hollow fiber membrane contactors,” *Sep. Purif. Technol.*, vol. 46, no. 1–2, pp. 33–40, Nov. 2005.

Wu J. and Chen V., “Shell-side mass transfer performance of randomly packed hollow fiber modules,” *J. Membr. Sci.*, vol. 172, no. 1–2, pp. 59–74, Jul. 2000.

Yan S., Fang M., Luo Z., and Cen K., “Regeneration of CO₂ from CO₂-rich alkanolamines solution by using reduced thickness and vacuum technology: Regeneration feasibility and characteristic of thin-layer solvent,” *Chem. Eng. Process. Process Intensif.*, vol. 48, no. 1, pp. 515–523, Jan. 2009.

Zhang H.-Y., Wang R., Liang D. T., and Tay, J. H. “Modeling and experimental study of CO₂ absorption in a hollow fiber membrane contactor,” *J. Membr. Sci.*, vol. 279, no. 1–2, pp. 301–310, 2006.

